

***K*-shell ionization of Ti, Fe, Ni, and Zn by 60–150-keV protons**

Arlen R. Zander and Mike C. Andrews III*

Physics Department, East Texas State University, Commerce, Texas 75428

(Received 24 April 1979)

K-shell ionization of thick targets of Ti, Fe, Ni, and Zn by 60–150-keV protons has been investigated. Experimental x-ray production cross sections have been determined as a function of proton energy. Absolute ionization cross sections are compared to predictions of the perturbed-stationary-state theory, including Coulomb deflection and approximate relativistic corrections (CPSSR). It is found that the CPSSR systematically overpredicts the values for the experimental data at the lower proton energies.

I. INTRODUCTION

In recent years, a great deal of effort has been devoted to the study of ionizing collisions produced by heavy ions impinging on target atoms (where "heavy" means with respect to the electron mass). In the case of slow-moving projectiles producing *K*-shell ionization by Coulomb excitation, the theoretical interpretations have undergone a continuous evolution. The first comprehensive formulation was the plane-wave Born approximation (PWBA) of Merzbacher and Lewis.¹ This was followed by the semiclassical formalism² and the binary-encounter approximation (BEA).³ The development of these theories and relevant data have been reviewed by Garcia *et al.*⁴ The BEA and PWBA both grossly overpredict the observed ionization cross sections at low projectile velocities where Coulomb deflection and binding effects are enhanced. Basbas *et al.*⁵ suggested modifications of the PWBA to take these effects into account. More recently,⁶ they have developed a perturbed-stationary-state formalism (PSS) in which binding and polarization effects are inherent. In the low-projectile-velocity regime, the PSS theory can be modified to account for Coulomb deflection and effects due to relativistic motion of the target electrons⁷ (CPSSR).

The proliferation of theoretical models has stimulated a wide variety of collision experiments designed to test the models. For the most part, these experiments have involved ions with energies above several hundred keV/amu incident on thin targets. In the case of incident protons, surveys^{8,9} of the literature indicate a paucity of experimental data at bombarding energies below 200 keV. This lack of attention may be attributed to several problems associated with measurements of x-ray yields for incident low-energy protons. Experimentally, target surface contaminations can produce erroneous results. Since thick targets must be utilized, data analysis is complicated by large uncertainties in determining the slope of

the x-ray excitation function. Additional uncertainties arise from lack of accurate stopping power information for low-energy protons. Typical errors associated with reported data in this low-velocity domain are on the order of 30%.

In spite of the problems involved, measurements of proton-induced ionization cross sections in the bombarding energy region below 200 keV are important. On the basis of the limited data available, this is precisely the domain where serious discrepancies between experimental results and theoretical predictions begin to appear. In this paper, we report experimental *K*-shell x-ray production cross sections for incident protons ranging in energy from 60–150 keV incident on targets of Ti, Fe, Ni, and Zn. The x-ray production cross sections are converted to ionization cross sections and compared to predictions of the CPSSR theory.

II. EXPERIMENTAL PROCEDURE

Thick (0.25 mm) targets of high-purity ($\geq 99.9\%$) Ti, Fe, Ni, and Zn were bombarded with a proton beam produced by the East Texas State University Cockcroft-Walton accelerator. The bombarding energy was varied from 60 to 150 keV in 10 keV increments. The accelerating voltage was determined using a 10^4 M Ω precision resistor chain. At the higher proton energies, the accelerating voltage was also verified from analyzing magnet settings for an H_2^+ beam at half the desired proton energy. Ion-source extraction voltages (≤ 500 V) were negligible compared to the acceleration voltage.

The number of incident protons was determined by direct current integration off the target holder which was electrically insulated from the rest of the experimental system. A negatively biased electron suppressor ring was used to prevent electron backstreaming from the target. An Ortec Model 439 current digitizer and a scalar were used to obtain numerical values for the integrated

charge. At all times the beam currents were maintained at levels low enough (1–10 μA) to minimize dead-time losses. The beam was focussed with a pair of electrostatic lenses and collimated to produce a 2-mm-diam beam spot on target.

The targets were mounted in a vacuum chamber on a target ladder positioned at 45° to both the incident beam direction and the central axis of the x-ray detector. In order to minimize surface contamination problems encountered in low-energy projectile studies, the targets were sputter-cleaned *in situ* prior to bombardment. This procedure consisted of pressurizing the target chamber to approximately 10^{-2} Torr with argon gas, biasing the target at -500 V with respect to a cold filament located inside the chamber, and maintaining a sputtering current of 50 mA for several minutes between the target and filament. During bombardment, the targets were also monitored visually through a glass port in one side of the target chamber to check for evidence of surface contamination. The pressure in the target chamber was maintained at 10^{-5} Torr or better throughout data acquisition. The characteristic x-rays emitted during proton bombardment passed through a 25.4- μm -thick Be window in one side of the target chamber before striking the x-ray detector.

The x rays were detected with a 30-mm² Nuclear Semiconductor Si(Li) detector placed at a distance of 8 cm from the target. The full width at half maximum resolution of the detector was 180 eV for 5.898-keV x rays. During operation, the detector was shielded with several layers of lead sheet. The effective efficiency of the detection system was determined using calibrated x-ray sources of ⁵¹Cr, ⁵⁴Mn, ⁵⁷Co, ⁶⁵Zn, and ²⁴¹Am together with standard procedures described by Gallagher and Cipolla.¹⁰ All sources utilized had a size consistent with the beam spot size and all were mounted in the same geometry maintained during experimental operation. The effective efficiency of the system takes into account the intrinsic efficiency of the Si crystal, the solid angle subtended by the Si(Li) detector, and attenuation losses of the emitted x rays in the Be windows on the target chamber and detector, in the air gap between the detector and target chamber, and in the gold surface layer and Si dead layer of the detector itself.

III. DATA ANALYSIS AND RESULTS

Experimental *K*-shell x-ray production cross sections σ_x were determined as a function of proton bombarding energy E from the standard thick-target-yield equation⁵

$$\sigma_x(E) = \frac{4\pi}{n\Omega\gamma} \left(\frac{dY}{dE} S(E) + \mu Y(E) \right), \quad (1)$$

where n is the number density of target atoms, Ω is the solid angle subtended at the target by the x-ray detector of efficiency γ , $S(E)$ is the stopping power of the target element for protons, μ is the absorption coefficient of the target for its own characteristic x-rays, and $Y(E)$ is the number of *K*-shell x rays detected per incident proton. The validity of Eq. (1) is based on the assumption of isotropic emission of the *K*-shell x rays¹¹ and the experimental geometry utilized.

The slope of the yield curve, dY/dE , was determined by fitting the experimental x-ray excitation function with polynomial, exponential, and power-law functions. Best results were obtained with a simple two-parameter power-law function of the form $Y(E) = aE^b$. This expression reproduced the experimental yields to within $\pm 15\%$ and contributed the largest error to our determination of σ_x .

The determination of accurate values for $S(E)$ was hampered by the wide range of experimental values reported in the literature and the fact that the proton energies utilized straddle the stopping-power maxima for the target elements studied.¹² The $S(E)$ values ultimately adopted were obtained from an interpolation formula suggested by Varelas and Biersack,¹³

$$S(E) = S_L S_H / (S_L + S_H), \quad (2)$$

where the low-energy stopping powers are given by¹²

$$S_L = A_1 E^{0.45} \quad (3)$$

and the high-energy ones by

$$S_H = (A_2/E) \ln(1 + A_3/E + A_4 E). \quad (4)$$

Values of the coefficients A_1 through A_4 were obtained from Ref. 12.

Values for the self-absorption coefficient μ were obtained from compilations by Veigele.¹⁴ In some instances, simple linear interpolations were used to obtain intermediate values of μ . Since the self-absorption term in Eq. (1) is essentially negligible for the elements studied, this method contributed no appreciable error to the calculated values of σ_x .

The principal contributions to the error in our measured values of σ_x are the uncertainties in the slope of the experimental yield curve and in the stopping power values. We assign uncertainties of $\pm 15\%$ to both of these quantities. Experimental uncertainties include a 2% error in the incident proton energy, 8% in the effective detection efficiency, 2% in charge integration, and 1%–4%

TABLE I. Proton-induced K -shell x-ray production cross sections as a function of proton energy. Column 1 lists the target element and its atomic number Z and K -shell fluorescence yield ω . Column 2 is the incident proton energy E . Column 3 is the x-ray production cross section $\sigma_x(E)$, in millibarns, as determined from Eq. (1). Column 4 lists other measured x-ray production cross sections. Column 5 lists the approximate relativistic correction factor R utilized in the CPSSR calculations.

Target	E (keV)	$\sigma_x(E)$ (mb)	Other $\sigma_x(E)$ (mb)	R
Ti	60	0.209		1.66
$Z=22$	70	0.616		1.55
$\omega=0.212$	80	1.57		1.46
	90	3.57	5.65 ^a	1.40
	100	7.45	8.98 ^b	1.35
	110	14.5	18.8 ^a	1.31
	120	26.4		1.28
	130	45.8	45.3 ^a	1.25
	140	76.3		1.23
	150	123	90.0, ^a 64.2 ^b	1.21
Fe	70	0.0285		2.18
$Z=26$	80	0.0816		2.00
$\omega=0.344$	90	0.206		1.87
	100	0.473	1.18 ^b	1.76
	110	0.995		1.68
	120	1.96		1.61
	130	3.66		1.55
	140	6.50	7.39 ^c	1.50
	150	11.1	12.1, ^b 10.5 ^c	1.46
Ni	80	0.0267		2.49
$Z=28$	90	0.0759		2.29
$\omega=0.414$	100	0.193	0.248 ^b	2.13
	110	0.448		2.00
	120	0.963		1.90
	130	1.95		1.81
	140	3.72		1.74
	150	6.81	4.55 ^b	1.68
Zn	100	0.0608		2.62
$Z=30$	110	0.134		2.43
$\omega=0.482$	120	0.274		2.28
	130	0.530		2.16
	140	0.973		2.06
	150	1.72		1.97

^aReference 15.

^bReference 16.

^cReference 17.

in measured yields at high and low bombarding energies respectively. We estimate our overall uncertainties in σ_x to be $\pm 30\%$ at the lower proton energies and slightly less at the higher energies.

Our experimental results for the K -shell x-ray production cross sections are presented in tabular form and compared to other measurements¹⁵⁻¹⁷ in Table I.

IV. COMPARISON TO THEORY

The CPSSR theory^{5,6} predicts that the K -shell ionization cross section σ_I , when properly scaled,

should exhibit a universal behavior governed by the function

$$F(\eta_K/\epsilon^2\theta_K^2) = \sigma_I \epsilon \theta_K / \sigma_0 9E_{10}(\pi dq_0 \epsilon), \quad (5)$$

where η_K and θ_K are proton-velocity and target-binding parameters, respectively, ϵ accounts for increased binding effects at low proton velocities, σ_0 is a scaling unit, the factor $9E_{10}(\pi dq_0 \epsilon)$ takes into account Coulomb deflection effects, and polarization effects are neglected. The solid curve shown in Fig. 1 represents the theoretical values of $F(\eta_K/\epsilon^2\theta_K^2)$ calculated from published tables.¹⁸

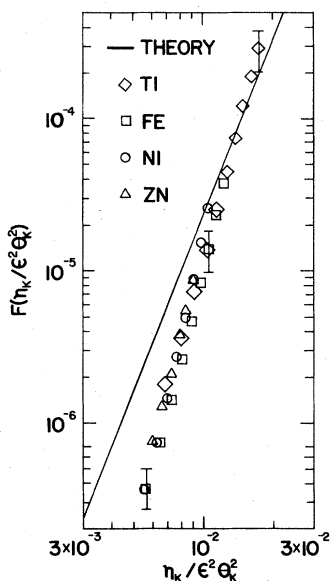


FIG. 1. Comparison of experimental and theoretical (CPSSR) values of the universal function $F(\eta_K/\epsilon^2\theta_K^2)$ defined by Eq. (5).

The measured K -shell x-ray production cross sections were converted to ionization cross sections according to the relation

$$\sigma_I = \sigma_x / \omega, \quad (6)$$

where the fluorescence yields ω listed in Table I were taken from Koustroun *et al.*¹⁹ These experimental ionization cross sections were then used in Eq. (5) together with the approximate relativistic correction factors⁷ R listed in Table I to calculate the experimental values of $F(\eta_K/\epsilon^2\theta_K^2)$ plotted in Fig. 1. The error bars shown in Fig. 1 represent only the 30% errors associated with our measurements of σ_x . They do not include any errors arising from uncertainties in the fluorescence yields.

The universal nature of the experimental data is evident from Fig. 1, but the CPSSR overpredicts the data at scaled energies below $\eta_K/\epsilon^2\theta_K^2 \approx 10^{-2}$. Furthermore, the trend appears to be toward even larger deviations at the lower energies. This observation is in agreement with the results of Shima²⁰ for lower- Z target elements and lower bombarding energies.

It should be noted that the effect of the approximate relativistic corrections incorporated into the CPSSR theory is to further increase the disagreement between theory and experiment. From Table I we see that the R factors by which the theoretical values are multiplied have their largest

values at the lowest proton energies. This result has been explained²¹ as being due to larger energy transfers occurring at lower bombarding energies. The fact that the simple multiplicative correction employed in the CPSSR formalism tends to enhance the discrepancy between theory and experiment suggests that it may be necessary to account for relativistic effects in a more sophisticated manner at lower projectile energies, perhaps through the use of relativistic electron wave functions.²²

Even without the approximate relativistic corrections utilized in the CPSSR theory, the deviations of the experimental data from the theoretical predictions still exceed experimental error for $\eta_K/\epsilon^2\theta_K^2 < 10^{-2}$. This discrepancy may be partially due to the fact that theoretical values for the universal function $F(\eta_K/\epsilon^2\theta_K^2)$ are obtained from tabulated²³ nonrelativistic PWBA calculations in which it is assumed that the energy transfer from the incident proton to the ejected electron is very small compared to the bombarding energy. If the exact value is used for the lower limit of the momentum transfer from the proton to the electron, the theoretical predictions are reduced by approximately 25% for the proton energies and target atoms investigated here.²⁴ From Fig. 1, it is clear that a much larger reduction of the theoretical values is required to remove the observed discrepancies between theoretical predictions and experimental results at the lower proton energies.

V. CONCLUSIONS

Observed proton-induced K -shell ionization cross sections at proton energies ≤ 150 keV exhibit a universal behavior when properly scaled. However, for reduced proton velocities corresponding to $\eta_K/\epsilon^2\theta_K^2 \leq 10^{-2}$, the CPSSR theory systematically overpredicts the observed values. Approximate relativistic correction factors in this domain are significant, but their inclusion in the CPSSR formalism increases the observed discrepancies. Incorporation of exact energy-transfer calculations into the CPSSR theory reduces the discrepancies somewhat but does not eliminate them. It appears that additional unknown factors affecting the ionization process must be included in the theory at low proton velocities.

ACKNOWLEDGMENTS

We wish to acknowledge valuable and enlightening discussions with G. Basbas and R. Rice. This research was supported in part by the Robert A. Welch Foundation and Research Corporation.

- *Present address: Dept. of Physics, North Texas State Univ., Denton, Tex. 76203.
- ¹E. Merzbacher and H. Lewis, in *Handbuch der Physik*, edited by S. Flügge (Springer-Verlag, Berlin, 1958), Vol. 34, p. 166.
- ²J. Bang and J. M. Hansteen, *K. Dan. Vidensk. Selsk. Mat.-Fys. Medd.* **31**, No. 13 (1959).
- ³J. D. Garcia, *Phys. Rev. A* **1**, 280 (1970); **1**, 1402 (1970); **4**, 955 (1971).
- ⁴J. D. Garcia, R. J. Fortner, and T. M. Kavanagh, *Rev. Mod. Phys.* **45**, 111 (1973).
- ⁵G. Basbas, W. Brandt, and R. Laubert, *Phys. Rev. A* **7**, 983 (1973).
- ⁶G. Basbas, W. Brandt, and R. Laubert, *Phys. Rev. A* **17**, 1655 (1978).
- ⁷J. S. Hansen, *Phys. Rev. A* **8**, 822 (1973).
- ⁸R. M. Wheeler, R. P. Chaturvedi, and A. R. Zander, in *Proceedings of the Third Conference on Applications of Small Accelerators, Denton, Texas, 1974*, edited by J. L. Duggan and I. L. Morgan (National Technical Information Service, Springfield, Va., 1974), Vol. I, p. 387.
- ⁹C. H. Rutledge and R. L. Watson, *At. Data Nucl. Data Tables* **12**, 195 (1973).
- ¹⁰W. H. Gallagher and S. Cipolla, *Nucl. Instrum. Methods* **405**, 122 (1974).
- ¹¹C. W. Lewis, R. L. Watson, and J. B. Natowitz, *Phys. Rev. A* **5**, 1773 (1972).
- ¹²H. H. Andersen and J. F. Ziegler, *Hydrogen Stopping Powers and Ranges in All Elements* (Pergamon, Elmsford, N.Y., 1977), Vol. 3.
- ¹³C. Varelas and J. Biersack, *Nucl. Instrum. Methods* **79**, 213 (1970).
- ¹⁴W. J. Veigele, *At. Data Tables* **5**, 51 (1973).
- ¹⁵K. Shima, I. Makino, and M. Sakisaka, *J. Phys. Soc. Jpn.* **30**, 611 (1971).
- ¹⁶J. L. Duggan, W. L. Beck, L. Albrecht, L. Munz, and J. D. Spaulding, in *Advances in X-Ray Analysis*, edited by K. F. J. Heinrich, C. S. Barrett, J. B. Newkirk, and C. O. Ruud (Plenum, New York, 1972), Vol. 15, p. 407.
- ¹⁷S. Messelt, *Nucl. Phys.* **5**, 435 (1958).
- ¹⁸R. Rice, G. Basbas, and F. D. McDaniel, *At. Data Nucl. Data Tables* **20**, 503 (1977).
- ¹⁹V. O. Kostroun, M. H. Chen, and B. Crasemann, *Phys. Rev. A* **3**, 533 (1971).
- ²⁰K. Shima, *Phys. Lett. A* **67**, 351 (1978).
- ²¹B. H. Choi, *Phys. Rev. A* **4**, 1002 (1971).
- ²²D. Jamnik and C. Zupančič, *K. Dan. Vidensk Selsk. Mat.-Fys. Medd.* **31**, No. 2 (1957).
- ²³G. S. Khandelwal, B. H. Choi, and E. Merzbacher, *At. Data* **1**, 103 (1969).
- ²⁴G. Basbas and R. Rice (private communication).